Published by Avanti Publishers

International Journal of Petroleum Technology

ISSN (online): 2409-787X

Reservoir Characterization Using Seismic Inversion Based on Sparse Layer Reflectivity and Hybrid Genetic Algorithms: A Comparative Case Study of Blackfoot, Canada

Nitin Verma[1], Ravi Kant[1], Raghav Singh[1], Satya P. Maurya[1,*], Gopal Hema[1], Ajay P. Singh[1] and Kumar H. Singh[2]

[1]*Department of Geophysics, Institute of Science, Banaras Hindu University, Varanasi 221005, India*

[2]*Department of Earth Sciences, Indian Institute of Technology, Mumbai 400076, India*

ARTICLE INFO

Article Type: Research Article

Academic Editor: Ahmed Naseem Al-Dawood

Keywords:
Sand channel
Pattern search
Seismic inversion
Genetic algorithm
Sparse layer reflectivity

Timeline:
Received: October 10, 2023
Accepted: November 28, 2023
Published: December 08, 2023

Citation: Verma N, Kant R, Singh R, Maurya SP, Hema GI, Singh AP, Singh KH. Reservoir characterization using seismic inversion based on sparse layer reflectivity and hybrid genetic algorithms: A comparative case study of Blackfoot, Canada. Int J Petrol Technol. 2023; 10: 151-162.

DOI: https://doi.org/10.15377/2409-787X.2023.10.11

ABSTRACT

This research paper introduces a comparative case study on reservoir characterization through seismic inversion techniques. The study specifically explores sparse layer reflectivity and a hybrid approach involving genetic algorithms and pattern search. The research assesses the effectiveness of these methodologies in delineating subsurface properties, with a particular focus on acoustic impedance. Through meticulous analysis, the paper aims to identify the strengths and limitations of each method, considering factors such as parameter estimation precision, computational efficiency, and adaptability to complex geological structures. The findings contribute valuable insights for selecting optimal seismic inversion techniques in reservoir characterization, advancing our understanding of how the integration of sparse layer reflectivity and hybrid genetic algorithms can enhance subsurface imaging accuracy and reliability. The results obtained from our inversion process significantly enhance the interpretation of seismic data by providing detailed insights into the subsurface. Both the sparse layer reflectivity (SLR) and hybrid genetic algorithm (HGA) algorithms have exhibited outstanding performance when applied to real datasets. The inverted impedance section reveals notable low acoustic impedance ranging from 8000 to 8500 m/s g/cc. This distinct zone, identified as a reservoir (sand channel), is located within the time interval of 1040–1065 ms. Our observations indicate that HGA demonstrates superior correlation results not only in the vicinity of well locations but also over a broader spatial range, suggesting its potential to provide higher-resolution outcomes compared to SLR.

*Corresponding Authors

Email: mauryasatya@bhu.ac.in
Tel: +(91) 9820851470

1. Introduction

Reservoir characterization is a pivotal aspect of petroleum exploration and production, essential for understanding subsurface properties and optimizing reservoir performance [1-4]. The application of seismic inversion plays a pivotal role in reservoir characterization and integrated exploration and reservoir studies, aiding in the identification of potential hydrocarbon reservoirs and reducing exploration costs and risks. Seismic inversion is a mathematical process utilized to estimate subsurface acoustic impedance in inter-well regions by leveraging seismic reflection data [5-6]. These parameters offer crucial insights into subsurface rock and fluid properties that seismic reflection data alone cannot provide, making accurate estimation imperative for obtaining clear subsurface information [6-8]. Among the diverse array of inversion methodologies, this research delves into the comparative assessment of two promising approaches such as sparse layer reflectivity and hybrid genetic algorithms. SLR employs local optimization and these methods represent a category of sophisticated seismic inversion techniques that contribute valuable insights into subsurface geological structures. These techniques prove especially effective in accurately predicting essential reservoir parameters, including acoustic impedance. By utilizing the reflectivity information inherent in seismic data, SLR inversion generates detailed and high-resolution images of the subsurface, thereby facilitating reservoir characterization and enhancing exploration endeavors [9-10]. In contrast, hybrid optimization, combining local and global optimization methods, emerges as a strategy to overcome the drawbacks of individual approaches. The proposed hybrid optimization algorithm in this study combines genetic algorithm and pattern search to achieve high-resolution subsurface acoustic impedance [11-13].

The methodology is evaluated real seismic data from the Blackfoot field in Alberta, Canada. The results demonstrate the efficiency of the SLR and hybrid optimization approach, especially in terms of accuracy and reduced computation time. This research embarks on a comprehensive case study, scrutinizing the performance of these techniques in reservoir characterization. The study aims to provide a nuanced understanding of the strengths and limitations associated with sparse layer reflectivity and hybrid genetic algorithms, considering factors such as precision in parameter estimation, computational efficiency, and adaptability to complex geological structures. Through this comparative analysis, the research contributes valuable insights that can guide the selection of optimal seismic inversion techniques, ultimately advancing our capabilities in subsurface imaging for reservoir characterization.

1.1. Study Area

The Blackfoot field, located in central Alberta, Canada, is renowned for its production of oil and gas extracted from the Glauconitic compound incised valley system. Similar to many other fields in Alberta, it significantly contributes to Canada's overall hydrocarbon output. The Western Canadian Sedimentary Basin, among the largest in North America, holds substantial reserves of hydrocarbons, including oil, natural gas, and oil sands. Fig. (**1**) illustrates the precise location of the study area. In 1996, seismic reflection data was collected through a survey conducted by Pan Canadian Petroleum and the Consortium for Research in Elastic-Wave Exploration Seismology. Geologically, the Blackfoot field is part of the Paleozoic sedimentary succession in the region, predominantly within the Lower Carboniferous (Mississippian-aged) Banff formation. This formation comprises carbonate rocks, such as limestone and dolomite. This study specifically utilizes seismic reflection data from the reef-prone glauconitic compound incised-valley system, employing 708 shots and 690 receivers. The recorded data has a frequency range of 5-90 Hz [14-16].

A glauconitic compound incised-valley system refers to a geological region where sedimentary deposits, rich in glauconite, serve as reservoir rocks for fossil fuels. In the Blackfoot Field, these incised valleys demonstrate a distinct geological pattern involving cyclical processes of filling and cutting. These cycles consist of the lower incised valley, the lithic incised valley, and the upper incised valley. Glauconite, a green mineral commonly found in marine environments, is recognized for its potential as a reservoir rock due to favorable porosity and permeability characteristics. The porosity and permeability of these reservoirs facilitate the storage and flow of hydrocarbons.

Effective reservoir characterization and hydrocarbon extraction in the Blackfoot Field hinge on understanding the spatial distribution, shape, and properties of the lower, upper, and lithic incised valleys. The reservoir at

Blackfoot Field is filled with glauconitic sand from the Lower Cretaceous Glauconitic deposit. The Glauconitic Formation in the Blackfoot Field, composed of sediments with a grain size ranging from fine to medium, acts as potential reservoir rocks. Glauconite, imparting a greenish tint to rocks, is commonly present in these sediments. The formation may also contain shale and sands with lacustrine and channel origins.

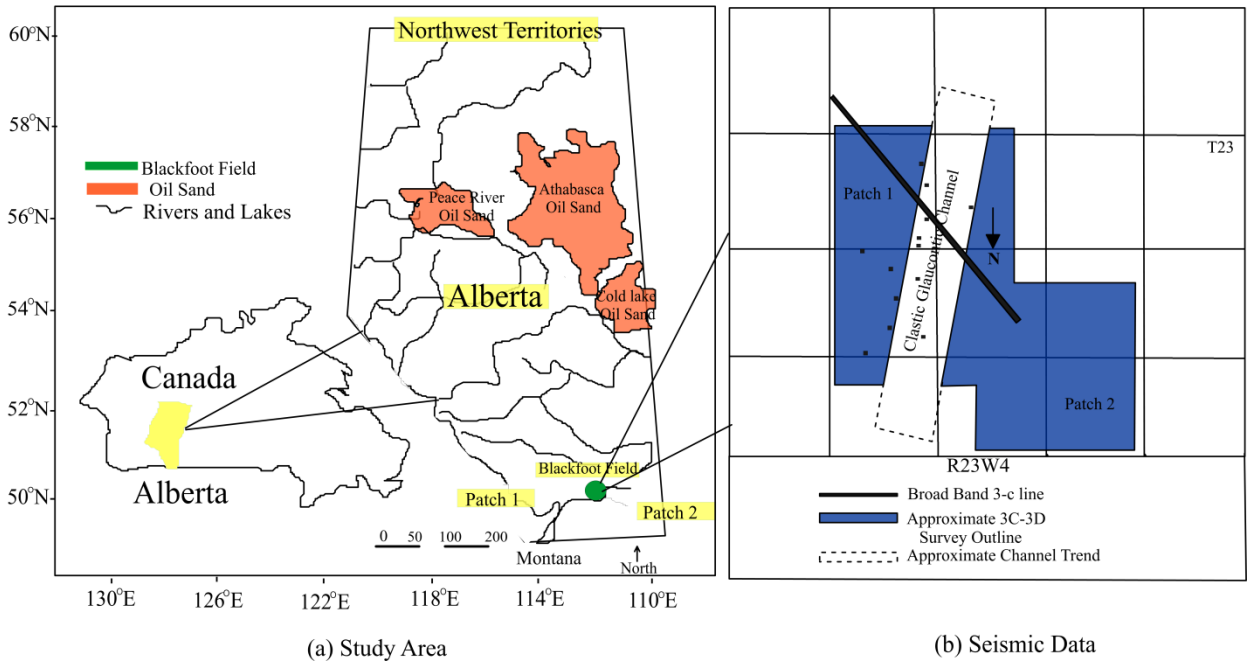

Figure 1: a) Map showing study area, the Blackfoot field, Alberta, Canada (highlighted by green circle) and **b**) depicts trend of seismic data with Glauconitic sand channel in the subsurface.

2. Methodology

2.1. Sparse Layer Reflectivity Inversion

Sparse Layer Reflectivity (SLR) inversion serves as a geophysical method employed for deducing subsurface characteristics, including acoustic impedance and porosity, from seismic data. This technique operates on the principle of modeling the reflectivity series of subsurface layers and iteratively adjusting the model to align with observed seismic data [17-21]. In this context, sparse layer reflectivity algorithms play a significant role in modeling and interpreting the reflectivity information obtained from seismic traces. The Earth's subsurface often exhibits sparse and layered structures, and these algorithms capitalize on this by incorporating sparsity into the inversion process. Sparsity implies that certain layers or zones contribute significantly to the observed seismic data, while others may not [22-24]. To achieve this, algorithms for sparse layer reflectivity often employ regularization methods such as L1 regularization or total variation regularization. These techniques encourage the inversion models to have many zero or near-zero values, resulting in solutions that emphasize essential subsurface features and improve interpretability [25]. The benefits of these algorithms include enhanced resolution and accuracy, particularly in cases where distinct layered structures exist. However, challenges, such as selecting appropriate regularization parameters, correct initial model and addressing non-uniqueness in the sparse layer reflectivity inversion process, need careful consideration, making this method suitable for cases where a simple interpretable geological model is desired [26-29].

2.2. Hybrid Optimizations

Hybrid optimization, particularly utilizing genetic algorithms (GA) and pattern search (PS), proves effective in mitigating drawbacks and improving results. GA is not reliant on the initial model and optimization process involves the evolution of a population of potential solutions over multiple generations. The algorithm starts with a

randomly generated population, and through selection, crossover, and mutation operations, it iteratively refines the solutions [30-34]. On the other hand PS is dependent on the initial model. It starts at a specific point in the solution space and systematically explores patterns or directions from that starting point. The effectiveness of pattern search can be influenced by the choice of the initial point and the patterns used for exploration [35-37]. A poor choice of the initial point may lead to suboptimal solutions, and the success of the algorithm is somewhat tied to the quality of the initial model. The present study addresses this challenge by introducing a methodology that integrates genetic algorithms and pattern search [38-44]. The approach involves providing a limited time for the genetic algorithm to obtain near-optimal results. Once proximity is achieved, local optimization methods, employing results from the genetic algorithm as an initial model, expedite convergence to the optimum solution. The rationale behind choosing GA as global optimization and PS as local optimization lies in their ease of implementation and lower expertise requirements. The steps in combining global and local optimization in this study include selecting seismic and well-log data, converting depth to time, implementing genetic operators to obtain an initial population, calculating reflectivity and synthetic traces, assessing RMS error between synthetic and input seismic data, and iteratively modifying the initial population to minimize RMS error within a limited time [45-46]. Subsequently, a pattern search algorithm is employed using the output of the genetic algorithm as the initial model. The process involves to calculating RMS error using equation (**3**), identifying the best solution. This iterative process continues until the program terminates, yielding the desired acoustic impedance.

$$\text{RMS Error (E)} = \frac{1}{n}\sqrt{\sum_{j=1}^{n}\left(S_{obs}^{i} - S_{mod}^{i}\right)^2} + \frac{1}{n}\sqrt{\sum_{j=1}^{n}\left(Z_{obs}^{i} - Z_{mod}^{i}\right)^2}$$

Where n is the total number of sample points, S_{obs}^{i} is input seismic data at the i^{th} sample, S_{mod}^{i} is the synthetic trace at the i^{th} sample. The other part of the equation is used here to constraints solution and this information comes from the prior study i.e. well–log in our case. Z_{obs}^{i} is the impedance at i^{th} sample estimated directly from well log data and Z_{mod}^{i} is the impedance at i^{th} sample generated by the genetic algorithm in its population.

In summary we can say that the sensitivity to the initial model, assumptions made in the inversion process, and simplicity of sparse layer reflectivity models might limit their ability to capture complex geological structures accurately. In contrast in the hybrid approach, GA can explore a large solution space and discover global optima where as PS algorithms can efficiently refine solutions locally, potentially leading to improved convergence and solution quality.

3. Well log Analysis

The proposed research aims to analyze well log data and statistically assess petrophysical parameters to identify potential zones for hydrocarbon accumulation at different depths. The Blackfoot field in Canada features numerous wells and 3D post-stack seismic reflection data. While the seismic data records crosslines from one to 119 and inlines from one to 81. Within this region, four wells—01-08 logs, 08-08 logs, 09-08 logs, and 11-08 logs—are identified based on seismic data. Fig. (**2**) illustrates anvelocity, density and acoustic impedance curve for all four wells in the time period 900-1100 ms. Fig. (**2**) indicates that the majority of wells show low velocity, density, and acoustic impedance within the range of 1040 to 1065 ms. Opting for this approach to define an area of interest proves beneficial, since we have availability of seismic data from 0 to 1300 ms two-way travel time. It is more favorable to invert the data exclusively within the specified zone (900-1100 ms) due to constraints in time and cost associated with inverting the complete datasets.

4. Results and Discussion

In this study, the focus was on utilizing sparse layer reflectivity and genetic algorithm for determining acoustic impedance from post-stack seismic data in Canada's Blackfoot field. Despite having access to the complete seismic volume, a specific cross-section at inline 1 and crosslines 1 to 50 was chosen due to extended convergence periods shown in Fig. (**3**). The original well-log data is initially recorded in depth (measured in meters),

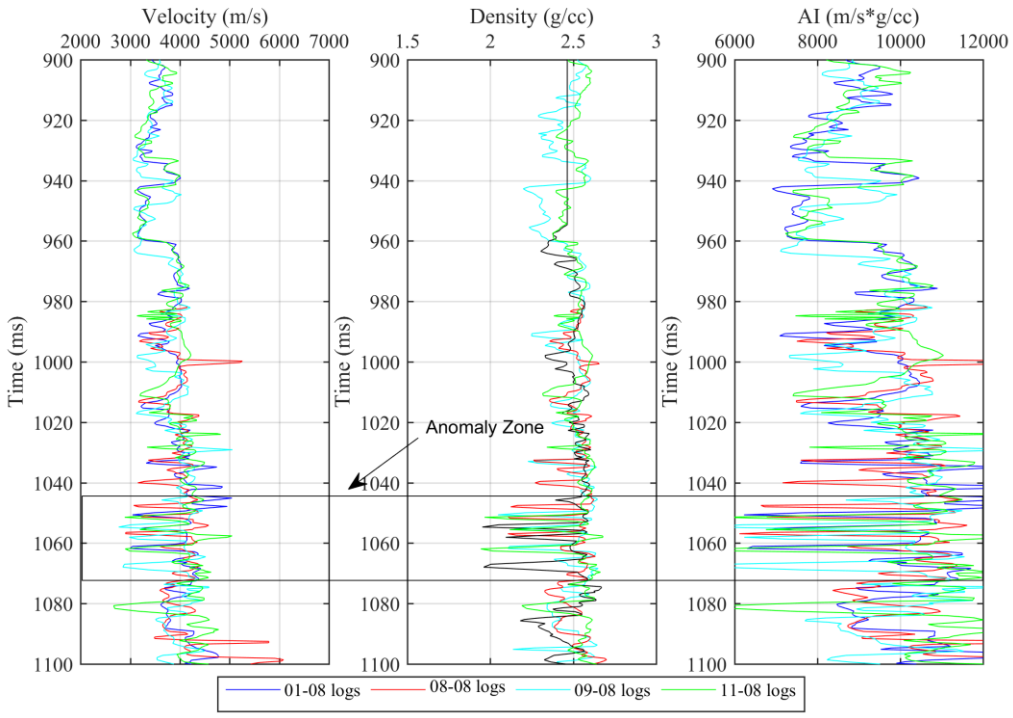

Figure 2: Petrophysical Analysis of wells 01-08, 08-08, 09-08, and 11-08, where (**a**) shows variation of (**a**) Velocity, (**b**) Density and (**c**) Impedance. The anomalous zone is highlighted with rectangle.

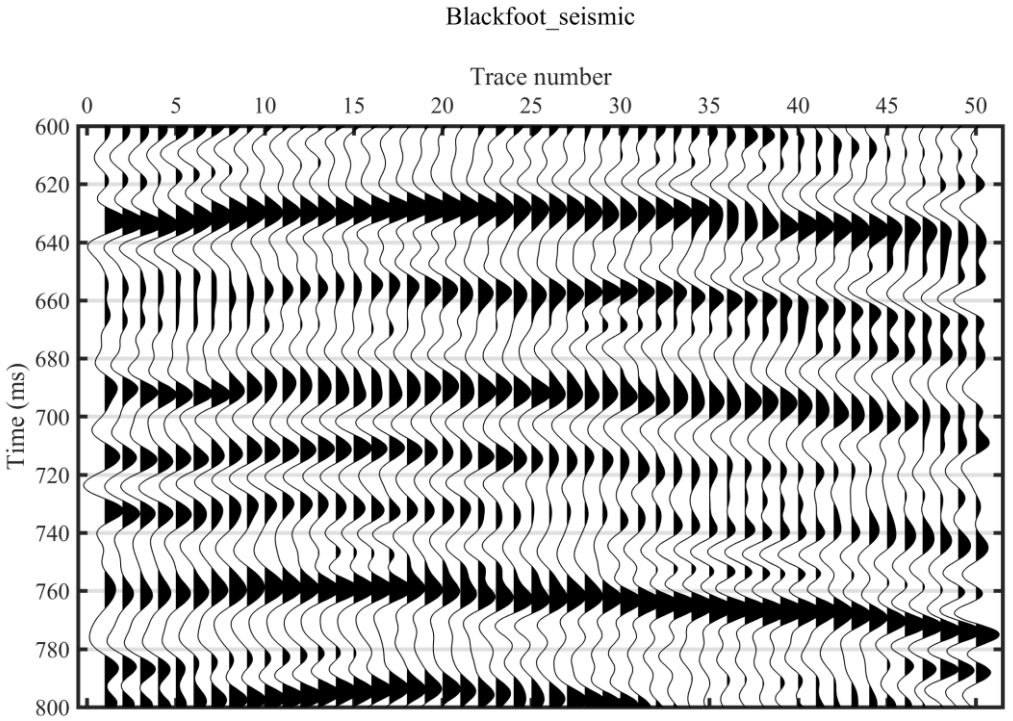

Figure 3: Post stack seismic section with time interval between 600 to 800ms.

while the analysis is conducted in the time domain. To facilitate alignment with seismic data, which is typically recorded in time, a depth-to-time conversion is carried out as illustrated in Fig. (**4**). In this figure, synthetic and composite traces are iteratively graphed multiple times, up to five repetitions. During this process, the synthetic trace undergoes adjustments, such as stretching or compressing, until a satisfactory peak-to-peak correlation is achieved with the composite trace. This iterative adjustment compensates for the difference in recording units

(depth versus time) and ensures precise alignment between the two datasets. This alignment is crucial for subsequent thorough analysis and interpretation. The p-impedance calculated at the well sites, as illustrated in Fig. (**5**), is subjected to interpolation to establish an initial impedance model for the acoustic impedance inversion. The examination of inversion at well sites serves as the initial phase in the seismic inversion procedure. The results obtained from the inversion analysis at well sites for both SLR and HGA demonstrate a commendable alignment between the all 4 well log (depicted in black) and the inverted impedance (depicted in red), as illustrated in Fig. (**6**). SLR exhibit average correlations of 0.86, 0.81, 0.85 and 0.86, where as HGA give 0.97, 0.93, 0.95 and 0.96 correlations between the well impedance and the inverted impedance. Additionally, an examination of the output results from the inversion process involves a cross plot that compares the original impedance with the predicted impedance, as depicted in Fig. (**7**) where the scatter data closely aligns with the best-fit line, indicating a close enough to each other between the inverted and well log impedances. Fig. (**8**) showcases the comparison of amplitude spectra between the seismic section and those derived from HGA and SLR. The two sets of amplitude spectra consistently demonstrate agreement across the entire frequency range, with notably high correlation coefficients of 0.99 and 0.89, respectively. Once again, HGA exhibits superior correlation compared to SLR. The

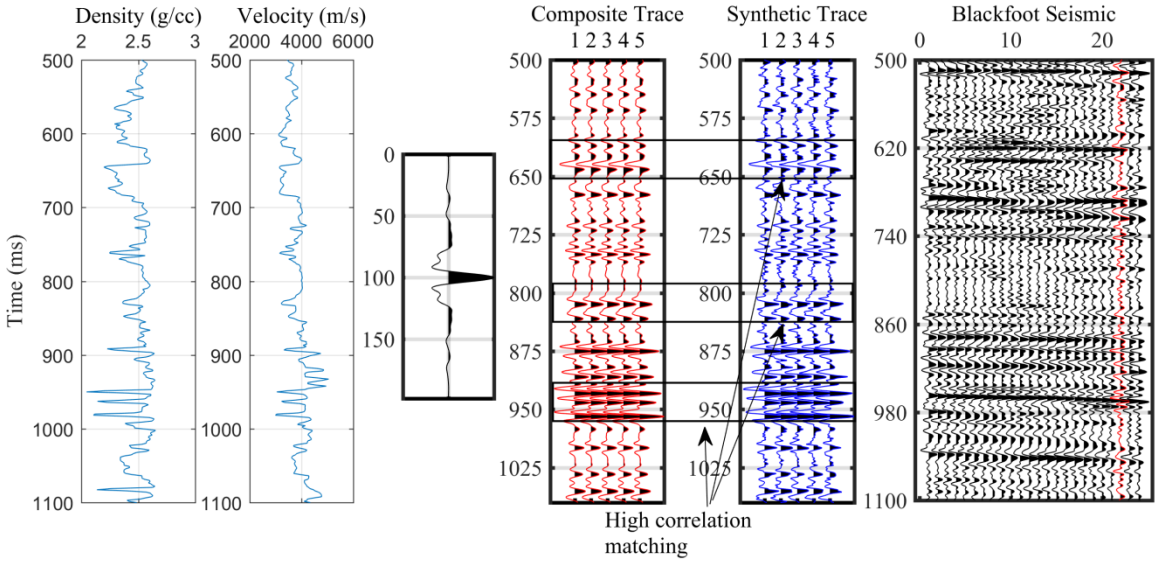

Figure 4: Seismic to well tie.

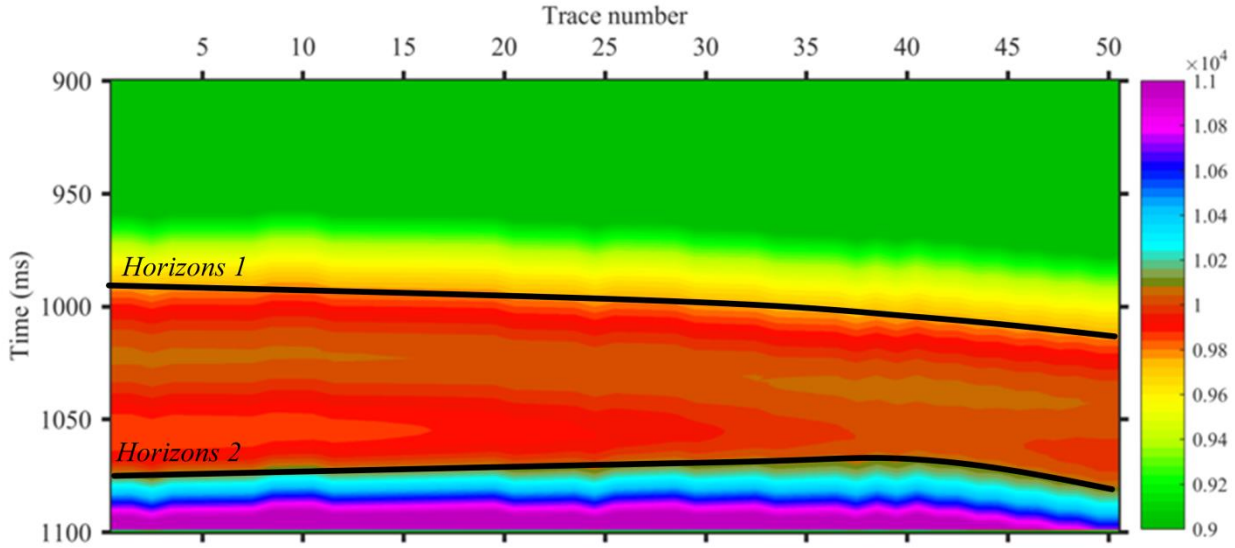

Figure 5: Low frequency model of impedance with two horizons.

composite analysis further emphasizes that HGA achieves a higher correlation value, with more data closely clustered around the best-fit line. The research findings suggest that the inverted results from HGA closely resemble the original impedance as compared to SLR.

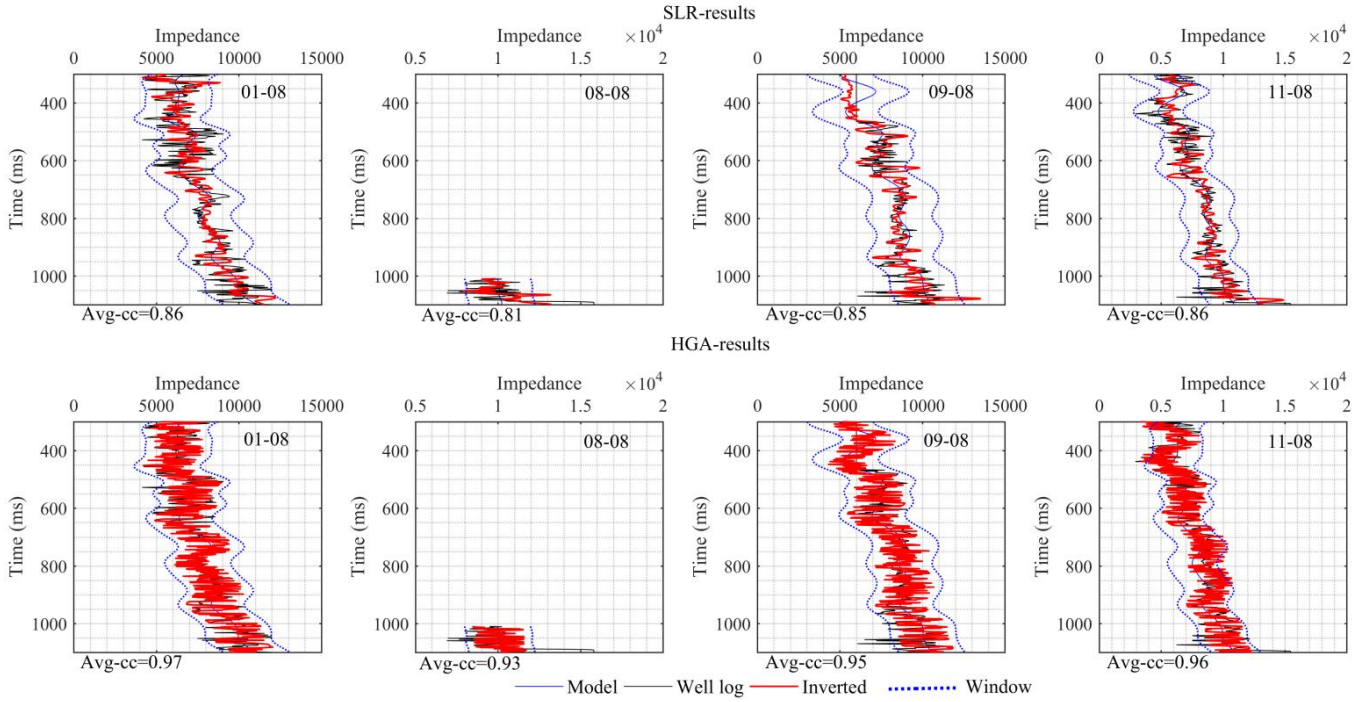

Figure 6: Compare the inverted impedance values with 01-08, 08-08, 09-08 and 11-08well log using SLR and HGA optimization. The first row presents the outcomes obtained through SLR, while the second row displays the results of HGA.

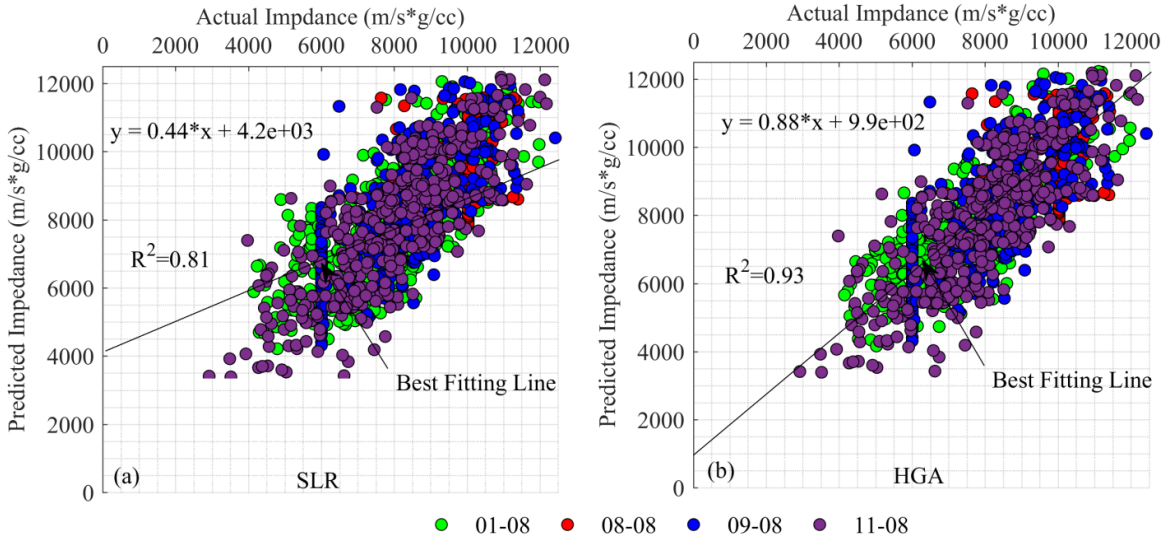

Figure 7: Cross plot between inverted and 4 well log impedance (**a**) generated from SLR (**b**) generated by HGA.

Now, the acoustic impedance inversion is extended to cover the entire seismic sections. The methodology, utilizing both SLR and HGA, is applied trace by trace to the Common Depth Point (CDP) stack segment. The cross-section, with a two-way travel duration ranging from 900 to 1100 milliseconds, is presented at inline 1 and crosslines 1 to 50. The high resolution achieved through CDP traces and the inversion technique accentuates a distinctive zone in the inverted image, possibly indicative of an interface between shale and sand, as evidenced by significant amplitude contrast and multiple strata in Fig. (**9a**). Fig. (**9b**,**9c**) specifically focus on the well site 01-08 logs, showcasing the inverted impedance derived from well-log data and the inverted impedance obtained from

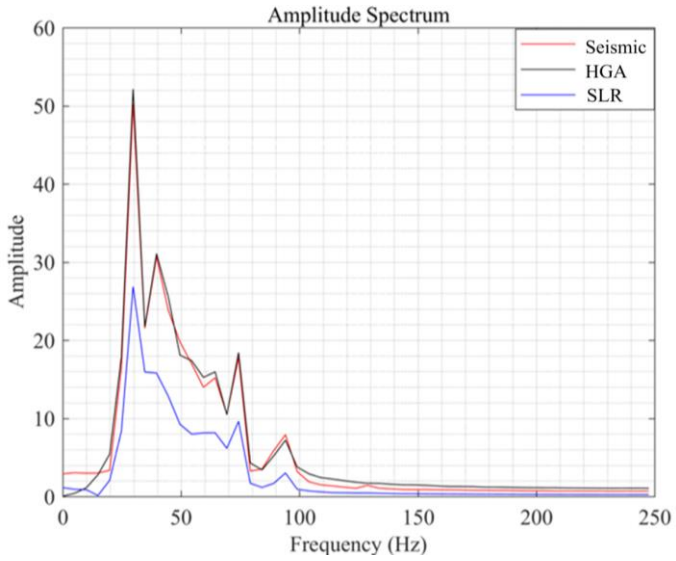

Figure 8: Compare the amplitude spectrum of seismic trace near the well 01-08 log to the synthetic traces which are generated by SLR and HGA inverted impedance.

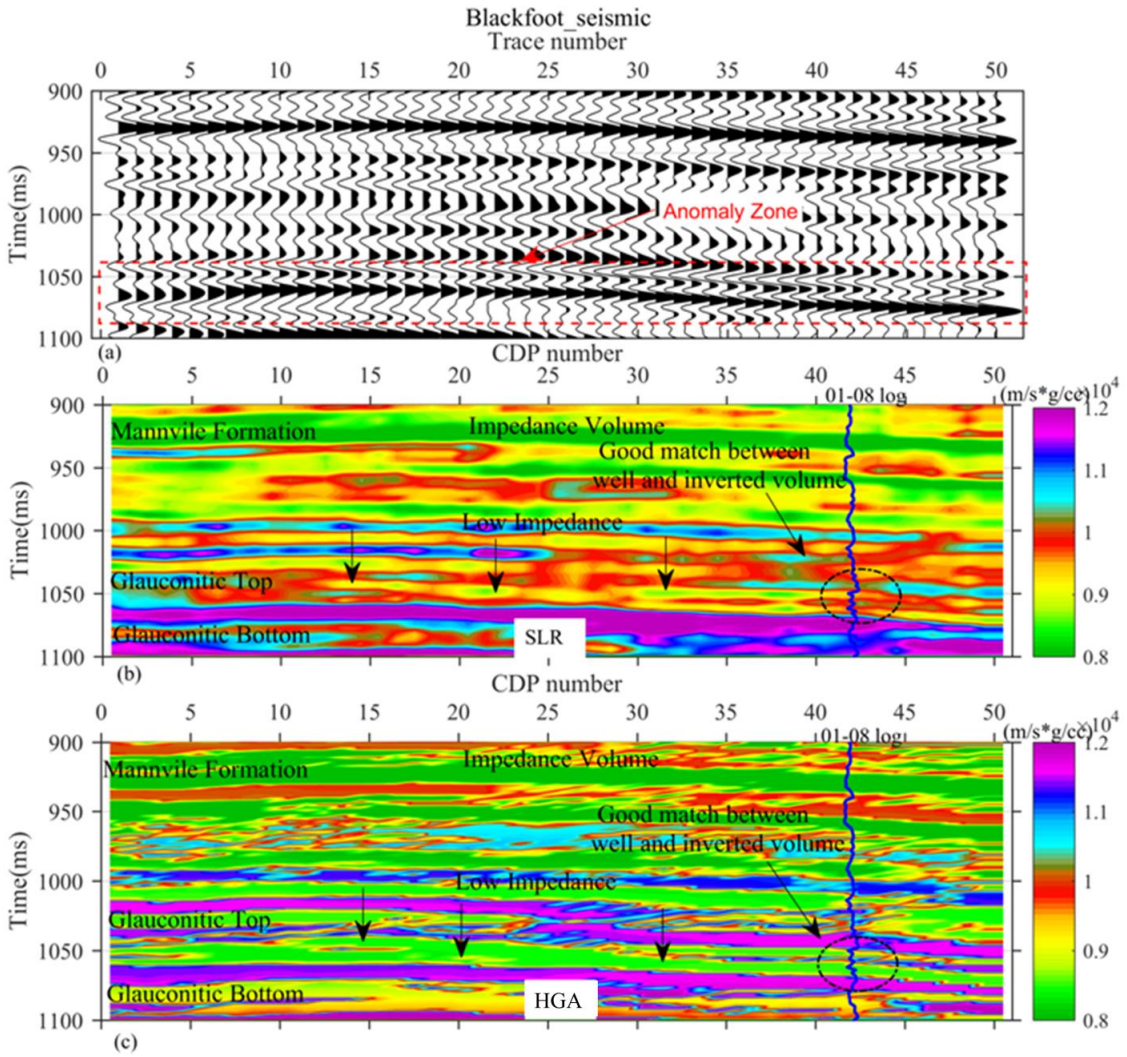

Figure 9: Inverted seismic volume with well 01-08 logs (**a**) seismic section, (**b**) Inverted impedance (SLR) and (**c**) Inverted impedance (HGA).

seismic data using the SLR and HGA approaches. The comparison highlights the striking similarity between the two sets of results, with the high impedance layer (>11,000 m/s*g/cc) surrounding the low impedance reservoir zone (ranging from 8,000 to 8,500 m/s*g/cc) on both sides, defining the border at 1040 ms as a highly reflecting layer. The inverted sections provide enhanced resolution and within-layer information compared to seismic data, which primarily offers interface information. The investigation of the inverted acoustic impedance volume reveals an anomalous low-AI zone between 1040 and 1065 TWT, suggesting the presence of a sandstone reservoir potentially filled with glauconitic minerals. This anomaly is closely associated with a seismic high amplitude anomaly, reinforcing the interpretation of this area as a sand channel. Fig. (**9**) effectively illustrates the region with low acoustic impedance, with HGA demonstrating higher subsurface resolution compared to SLR.

Further assessment involved comparing real seismic traces with inverted synthetic traces generated through forward modeling. Both SLR and HGA methods demonstrated remarkable similarity between Blackfoot seismic and reconstructed synthetic data shown in Fig. (**10**). Fig. (**10**) is divided into two panels for comparative analysis. In the first panel, the SLR method is employed to compare Blackfoot seismic data with replicated synthetic seismic. Meanwhile, the second panel utilizes the HGA method for the difference between actual seismic traces and the traces obtained through inversion. The correlation between original trace and synthetic trace is 0.86 and 0.98 respectively. Quantitatively, HGA consistently outperformed SLR, showcasing higher correlation coefficients. In conclusion, the practical application of SLR and HGA in seismic inversion for real data in the Blackfoot field demonstrated the effectiveness of these techniques in accurately determining acoustic impedance and identifying subsurface features. The results consistently favored HGA over SLR in terms of correlation and resolution, highlighting the potential of these methods in enhancing subsurface characterization in oil and gas exploration.

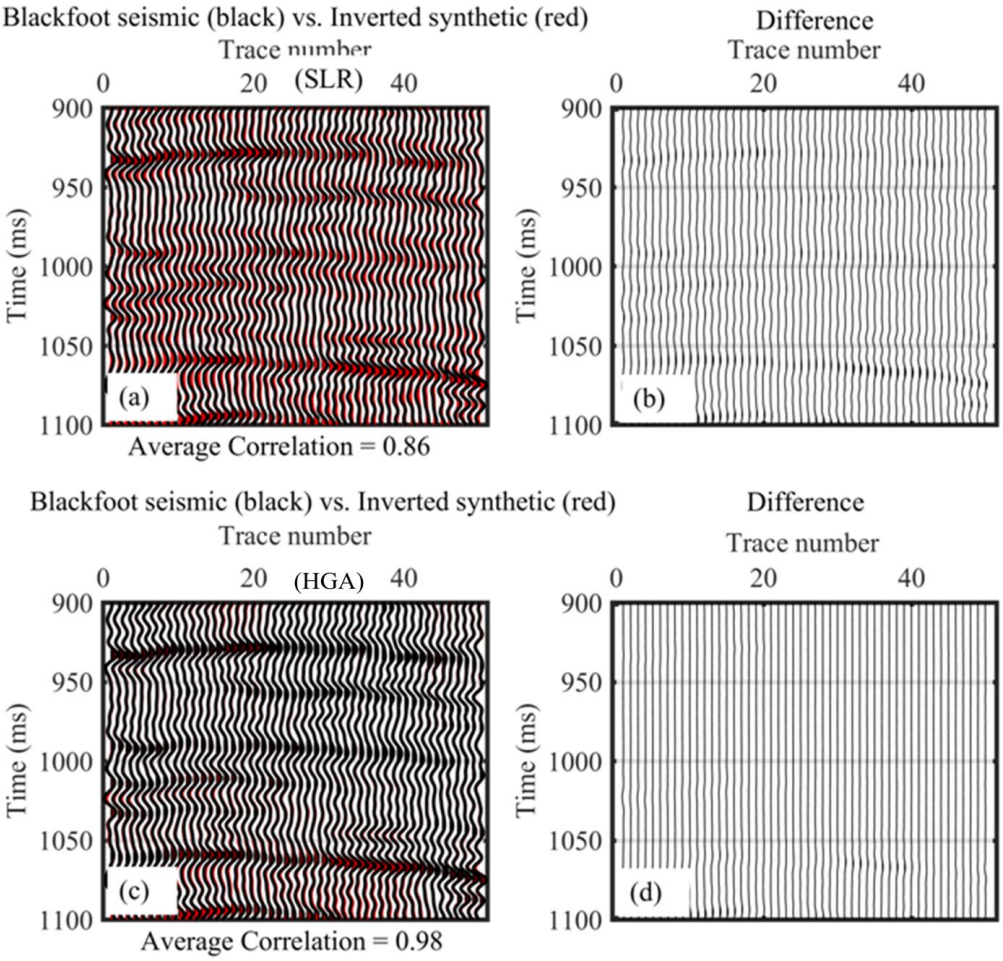

Figure 10: Cross-section compares reproduced synthetic from inverted impedance section and Blackfoot seismic section (left) along with their difference (right).

In order to validate the accuracy of the obtained results from SLR and HGA assisted by seismic attributes, a cross-validation process is conducted. Seismic attributes, which are quantitative measurements derived from seismic data, play a crucial role in providing key information about subsurface geology and are integral to the exploration and production of hydrocarbon reservoirs. Among these attributes, the amplitude envelope stands out as particularly valuable. It serves to highlight variations in seismic data and offers a meaningful indication of changes in seismic amplitudes, especially in regions where high amplitude zones align with low impedance zones within the same time interval, as depicted in Fig. (**11**). This enhancement facilitates the identification of specific geological features such as boundaries between rock layers, fault zones, and potential reservoirs. Consequently, the amplitude envelope proves to be an essential seismic attribute for tasks like reservoir characterization, geological interpretation, and the mapping of subsurface structures within the oil and gas industry.

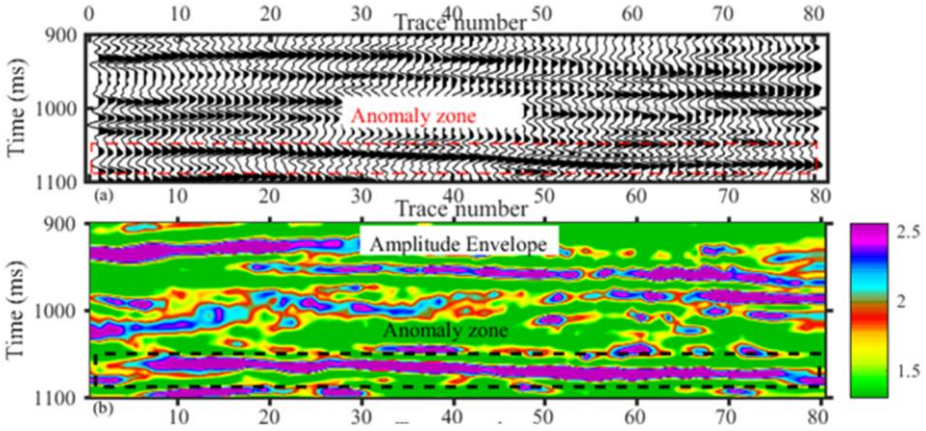

Figure 11: a) Blackfoot seismic traces, **b**) amplitude envelope attributes.

5. Conclusion

The developed flowchart for seismic inversion using HGA and SLR underwent rigorous evaluation with both synthetic and real data. Significantly, HGA consistently outperformed SLR across various well locations, showcasing its superiority not only at well log sites but also on a broader scale. The inverted impedance and predicted porosity models achieved unprecedented subsurface detail, capturing variations in impedance (8000 to 12000 m/s g/cc) and also the HGA requires 48 seconds to invert a single trace of real data, while SLR takes 26 seconds for the same task. Our analysis revealed a distinctive anomaly, characterized by low impedance (8000 to 8500 m/s g/cc), within the time range of 1040–1065 ms two-way travel times. Crucially, this anomaly aligns with observed reservoir characteristics in well-log data. Based on our findings, we strongly advocate for the preference of HGA over SLR in exploration and production (E&P) projects, as HGA consistently provides high-resolution subsurface data.

Conflict of Interest

The authors declare that there is no conflict of interest.

Funding

The authors, Dr. S.P. Maurya, expresses gratitude to the funding organizations UGC-BSR (M-14-0585) and IoE BHU (Dev. Scheme no. 6031B) for their financial assistance.

Acknowledgments

We thank GeoSoftware for providing Hampson Russell software, particularly Emerge, and Geoview. In addition, we acknowledge the academic licenses for Matlab (2022b) and Norsar (full package), respectively, from www.mathworks.com and www.norsar.no respectively. This work could not be done without their help.

Availability of Data and Materials

Not applicable.

References

[1] Li XY, Zhang YG. Seismic reservoir characterization: how can multicomponent data help? J Geophys Eng. 2011; 8: 123-141. https://doi.org/10.1088/1742-2132/8/2/001

[2] Partyka G, Gridley J, Lopez J. Interpretational applications of spectral decomposition in reservoir characterization. The Leading Edge. 1999; 18(3): 353-60. https://doi.org/10.1190/1.1438295

[3] Doyen P. Seismic reservoir characterization: An earth modelling perspective (EET 2). EAGE Publications; 2007. https://doi.org/10.3997/9789462820234

[4] Maxwell SC, Rutledge J, Jones R, Fehler M. Petroleum reservoir characterization using downhole microseismic monitoring. Geophysics. 2010; 75(5): 75A129-37. https://doi.org/10.1190/1.3477966

[5] Pendrel J. Seismic inversion—the best tool for reservoir characterization. CSEG Rec. 2001; 26, 18-24.

[6] Sokolov A, Schulte B, Shalaby H, van der Molen M. Seismic inversion for reservoir characterization. In Onajite E, Ed. Applied techniques to integrated oil and gas reservoir characterization. Elsevier; 2021, pp. 329-51. https://doi.org/10.1016/B978-0-12-817236-0.00013-3

[7] Sen Mrinal K, Society of Petroleum Engineers (U.S.). Seismic inversion. Richardson, Tex.: Society of Petroleum Engineers; 2006.

[8] Maurya S, Singh K, Kumar A, Singh N. Reservoir characterization using post-stack seismic inversion techniques based on real coded genetic algorithm. J Geophys. 2018; 39: 95-103.

[9] Zhang R, Castagna J. Seismic sparse-layer reflectivity inversion using basis pursuit decomposition. Geophysics. 2011; 76(6), 147-58. https://doi.org/10.1190/geo2011-0103.1

[10] Russell B, Downton J, Colwell T. Sparse layer reflectivity with FISTA for post-stack impedance inversion. EAGE Conference 2020; pp. 1-5. https://doi.org/10.3997/2214-4609.202037018

[11] Velez-Langs O. Genetic algorithms in the oil industry: An overview. J Pet Sci Eng. 2005; 47, 15-22. https://doi.org/10.1016/j.petrol.2004.11.006

[12] Soupios P, Akca I, Mpogiatzis P, Basokur AT, Papazachos C. Applications of hybrid genetic algorithms in seismic tomography. J Appl Geophys. 2011; 75(3): 479-89. https://doi.org/10.1016/j.jappgeo.2011.08.005

[13] Junyu B, Zilong X, Yunfei X, Tianshou X. Nonlinear hybrid optimization algorithm for seismic impedance inversion. In Beijing 2014 International Geophysical Conference & Exposition, Beijing, China: SEG & CPS; 21-24 April 2014; pp. 541-4. https://doi.org/10.1190/IGCBeijing2014-138

[14] Maurya SP, Sarkar P. Comparison of post stack seismic inversion methods: a case study from Blackfoot field, Canada. Int J Eng Res. 2016; 7(8): 1091-101

[15] Lawton DC, Robert RS, Andreas C, Stacey H. Advances in 3C–3D design for converted waves. CREWES Res Rep. 1996; 7: 43-51.

[16] Lawton DC, Stewart R, Cordsen A, Hrycak S. Design review of the Blackfoot 3C-3D seismic program. CREWES Res Rep. 1996; 8(38): 1-38.

[17] Maurya SP, Singh NP. Application of LP and ML sparse spike inversion with probabilistic neural network to classify reservoir facies distribution-A case study from the Blackfoot field, Canada. J Appl Geophys. 2018; 159: 511-21. https://doi.org/10.1016/j.jappgeo.2018.09.026

[18] Dufour J, Squires J, Goodway WN, Edmunds A, Shook I Case History: Integrated geological and geophysical interpretation case study, and Lamé rock parameter extractions using AVO analysis on the Blackfoot 3C-3D seismic data, southern Alberta, Canada. Geophysics.2002; 67(1): 27-37.https://doi.org/10.1190/1.1451319

[19] Chopra S, Castagna J, Portniaguine O Seismic resolution and thin-bed reflectivity inversion. CSEG Rec. 2006; 31(1): 19-25

[20] Chai X, Wang S, Yuan S, Zhao J, Sun L, Wei X Sparse reflectivity inversion for nonstationary seismic data. Geophysics.2014; 79(3): V93-V105

[21] Palo P, Panda SS, Mandai R, Routray A Sparse layer inversion using linear programming approach. In: IGARSS 2019-2019 IEEE international geoscience and remote sensing symposium, 2019; 1923-6.

[22] Hampson D, Todorov T, Russell B. Using multi-attribute transforms to predict log properties from seismic data. Explor Geophys. 2000; 3: 481-7. https://doi.org/10.1071/EG00481

[23] Maurya SP, Singh NP, Singh KH. Seismic inversion methods: a practical approach. Springer Cham; 2020. https://doi.org/10.1007/978-3-030-45662-7

[24] Roth G, Tarantola A. Neural networks and inversion of seismic data. J Geophys Res. 1994; 99(B4): 6753-68. https://doi.org/10.1029/93JB01563

[25] Bosch, Miguel, Tapan Mukerji, and Ezequiel F. Gonzalez. Seismic inversion for reservoir properties combining statistical rock physics and geostatistics: A review. Geophysics. 2010; 75(5): 75A165-75A176.https://doi.org/10.1190/1.3478209

[26] Pendrel J. Seismic inversion—The best tool for reservoir characterization. CSEG Recorder. 2001; 26(1): 18-24.

[27] Pendrel J. Seismic inversion–still the best tool for reservoir characterization. CSEG Recorder. 2006; 31(1): 5-12.

[28] Artun E, Mohaghegh SD, Toro J, Wilson T, Sanchez A. Reservoir characterization using intelligent seismic inversion. SPE Eastern Regional Meeting, Morgantown, West Virginia: SPE; 14-16 September 2005. https://doi.org/10.2118/98012-MS

[29] Helland-Hansen D, Magnus I, Edvardsen A, Hansen E. Seismic inversion for reservoir characterization and well planning in the Snorre Field. Lead Edge. 1997; 16(3): 269-74. https://doi.org/10.1190/1.1437616

[30] Boschetti F, Dentith MC, Ron D. Inversion of seismic refraction data using genetic algorithms. Geophysics. 1996; 61(6): 1715-27. https://doi.org/10.1190/1.1444089

[31] Stoffa PL, Sen MK. Nonlinear multiparameter optimization using genetic algorithms; inversion of plane-wave seismograms. Geophysics.1991; 56(11): 1794-1810. https://doi.org/10.1190/1.1442992

[32] Louis SJ, Chen Q, Pullammanappallil S. Seismic velocity inversion with genetic algorithms. Proceedings of the 1999 Congress on Evolutionary Computation-CEC99 (Cat. No. 99TH8406), Washington, DC, USA: 1999, pp. 855-61. https://doi.org/10.1109/CEC.1999.782512

[33] Yamanaka, Hiroaki, and Hiroshi Ishida. Application of genetic algorithms to an inversion of surface-wave dispersion data. Bull Seismol Soc Am.1996; 86(2): 436-44. https://doi.org/10.1785/BSSA0860020436

[34] Gerstoft P. Inversion of seismoacoustic data using genetic algorithms and a posteriori probability distribution. J Acoust Soc Am.1994; 95(2): 770-82. https://doi.org/10.1121/1.408387

[35] da Silva Pereira JE, Strieder AJ, Amador JP, da Silva JLS, Descovi Filho LLV. A heuristic algorithm for pattern identification in large multivariate analysis of geophysical data sets. Comput Geosci. 2010; 36(1): 83-90. https://doi.org/10.1016/j.cageo.2009.03.009

[36] Song X, Gu H, Zhang X, Liu J. Pattern search algorithms for nonlinear inversion of high-frequency Rayleigh-wave dispersion curves. Comput Geosci. 2008; 34(6): 611-24. https://doi.org/10.1016/j.cageo.2007.05.019

[37] Song X, Li D, Gu H, Liao Y, Ren D. Insights into performance of pattern search algorithms for high-frequency surface wave analysis. Comput Geosci. 2009; 35(8): 1603-19. https://doi.org/10.1016/j.cageo.2009.01.007

[38] Bagheripour P, Asoodeh M. Fuzzy ruling between core porosity and petrophysical logs: Subtractive clustering vs. genetic algorithm–pattern search. Int J Geosci. 2013; 99: 35-41. https://doi.org/10.1016/j.jappgeo.2013.09.014

[39] Song X. Pattern Search Algorithms for Surface Wave Analysis. In Mansour N, Ed., Search Algorithms and Applications. Intech Open; 2011. https://doi.org/10.5772/14902

[40] Chunduru RK, Sen MK, Stoffa PL. Hybrid optimization methods for geophysical inversion. Geophysics.1997; 62(4): 1196-207. https://doi.org/10.1190/1.1444220

[41] Krahenbuhl, Richard A, Li Y. Hybrid optimization for lithologic inversion and time-lapse monitoring using a binary formulation. Geophysics. 2009; 74: 155-65. https://doi.org/10.1190/1.3242271

[42] Ji Y, Singh SC. Anisotropy from full waveform inversion of multicomponent seismic data using a hybrid optimization method. Geophys Prospect. 2005; 53: 435-45. https://doi.org/10.1111/j.1365-2478.2005.00476.x

[43] Giannakis I, Tsourlos P, Papazachos C, Vargemezis G, Giannopoulos A, Papadopoulos N, *et al*. A hybrid optimization scheme for self-potential measurements due to multiple sheet-like bodies in arbitrary 2D resistivity distributions. Geophys Prospect. 2019; 67(7): 1948-64. https://doi.org/10.1111/1365-2478.12793

[44] Zhao Z, Sen MK. A hybrid optimization method for full-waveform inversion. SEG/AAPG/SEPM First International Meeting for Applied Geoscience & Energy, Denver, Colorado, USA: SEG; September 2021. https://doi.org/10.1190/segam2021-3594393.1

[45] Singh R, Srivastava A, Kant R, Maurya SP, Mahadasu P, Verma N, *et al*. Integrated thin layer classification and reservoir characterization using sparse layer reflectivity inversion and radial basis function neural network: a case study. Mar Geophys Res. 2024; 45: 3. https://doi.org/10.1007/s11001-023-09537-w

[46] Verma N, Maurya SP, Singh KH, Singh R, Singh AP, Hema G, *et al*. Comparison of neural networks techniques to predict subsurface parameters based on seismic inversion: a machine learning approach. Earth Sci Inform. 2024; 1-22. https://doi.org/10.1007/s12145-023-01199-x